

Both protein-coding gene families and noncoding small RNA families are often analyzed with gene trees in molecular evolution research. Studies of gene families in any group of angiosperms can now use genes from *Amborella* as an outgroup (a reference for determining evolutionary relationships) in the analyses.

The *Amborella* genome provides clear structural evidence for an angiosperm-specific whole-genome duplication, which was previously inferred based on other data (5). It also provides additional evidence for the timing of that event at the branch leading to angiosperms in phylogenetic trees.

The *Amborella* genome sequence permitted reconstruction of the ancestral gene order in core eudicots by comparison to three eudicot genomes (grape, peach, and cacao). The hypothetical structure of seven inferred chromosomes in the ancestor of the core eudicots was reconstructed. Note that this was aided by the absence of an additional whole-genome duplication specific to the *Amborella* lineage. The ancestral eudicot genome reconstruction is useful for understanding how genomes have evolved in eudicots, which represent about 75% of angiosperm diversity. The ancestral eudicot genome reconstruction also will indicate how genome evolution has proceeded in different lineages after genome doubling (the gamma hexaploidy event) occurred early in eudicot evolution (6, 7).

Transposable elements in the *Amborella* genome are ancient, some of them having persisted for millions of years, but are no longer active. This is in contrast to many other angiosperm genomes in which transposable elements have proliferated, sometimes massively. The lack of transposable element activity in the *Amborella* genome may be due to very effective silencing mechanisms that prevent gene expression or the loss of active transposases that catalyze their movement (2); both could minimize or prevent their spread in the genome.

There are fewer than 15 known populations of *Amborella* in the world. Sequencing the genomes of 12 plants across this range revealed four genetically distinct clusters of populations and dynamic genome evolution. Despite its restricted geographic distribution, *Amborella* maintains substantial genetic diversity. Knowledge of genetic population structure may be helpful for guiding conservation efforts.

Large nuclear genomes from nonmodel eukaryotes are extremely challenging to assemble from relatively short sequencing reads derived from ultrahigh-through-

put sequencing (“next generation”) technologies. Chamala *et al.* used a new strategy to aid assembly (and its validation) that includes fluorescence in situ hybridization (FISH) to localize sequences by microscopy. Assembled chunks of the *Amborella* genome (scaffolds), representing about 68% of the assembled genome, were localized cytologically by FISH to assess their integrity and location on the chromosomes. The authors also used whole-genome mapping to help close gaps between scaffolds. This combined approach of shotgun sequencing, whole-genome mapping, and validation using FISH can be applied to other nonmodel organisms.

Rice *et al.* show that *Amborella* has one of the largest sequenced angiosperm mitochondrial genomes with five circular chromosomes. It contains a large amount of DNA that was transferred from other organisms, including mosses, flowering plants, and green algae. Some of the horizontally transferred genes were previously identified (8) but Rice *et al.* discovered and thoroughly characterized very large foreign regions including four whole-genome transfers. Horizontal transfer in *Amborella* may have been facilitated by its close association with other plants (epiphytes). Rice *et al.* propose a model whereby whole mitochondria were

captured and fused with the mitochondria of *Amborella*, after which genome recombination occurred. A low rate of mitochondrial DNA loss probably contributes to large horizontally transferred regions remaining in the genome for millions of years.

The sequencing, assembly, and analyses of the *Amborella* nuclear genome provide major insights into nuclear genome evolution in angiosperms and the kinds of genome features that were present in ancestral angiosperms. The information will be a useful resource for studies of genome evolution, gene family evolution, and phylogenetics.

#### References and Notes

1. D. E. Soltis *et al.*, *Am. J. Bot.* **98**, 704 (2011).
2. *Amborella* Genome Project, *Science* **342**, 1241089 (2013).
3. D. W. Rice *et al.*, *Science* **342**, 1468 (2013).
4. S. Chamala *et al.*, *Science* **342**, 1516 (2013).
5. Y. Jiao *et al.*, *Nature* **473**, 97 (2011).
6. Y. Jiao *et al.*, *Genome Biol.* **13**, R3 (2012).
7. D. Vekemans *et al.*, *Mol. Biol. Evol.* **29**, 3793 (2012).
8. U. Bergthorsson, A. O. Richardson, G. J. Young, L. R. Goertzen, J. D. Palmer, *Proc. Natl. Acad. Sci. U.S.A.* **101**, 17747 (2004).

**Acknowledgments:** K.A. is supported by the Natural Science and Engineering Research Council of Canada.

10.1126/science.1248709

## BIOCHEMISTRY

# Enzyme Kinetics, Past and Present

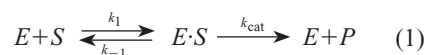
X. Sunney Xie

The Michaelis-Menten equation, first reported 100 years ago, holds at the single-molecule level.

Enzymes catalyze biochemical reactions, speeding up the conversion from substrate to product molecules. One hundred years ago, Leonor Michaelis and Maud Leonora Menten studied the equation characterizing enzymatic rates (1). This landmark development in the quantitative description of enzymes has stood the test of time, and the Michaelis-Menten equation remains the fundamental equation in enzyme kinetics (2). Today, the quest for fundamental understanding of the working of enzymes continues with vigor at the single-molecule level as new experiments and

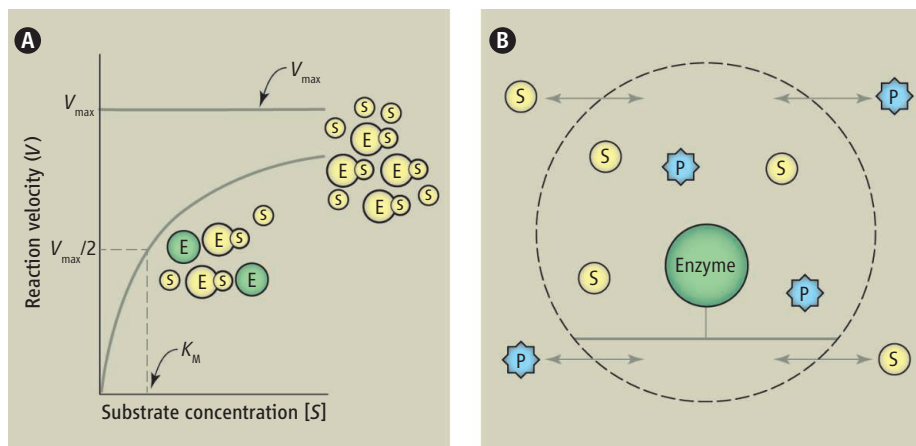
theories emerge.

Michaelis and Menten’s theory is not about how an enzyme speeds up a reaction. Rather, it describes a kinetic scheme for the enzyme *E* and its substrate molecule *S* to form a complex before proceeding to the product *P*:



where  $k_1$  and  $k_{-1}$  are the forward and reverse rate constants for substrate binding and  $k_{\text{cat}}$  is the catalytic rate constant. Assuming a fast equilibrium between *E* and *E*·*S*, they characterized the initial turnover rate of an enzyme, *V*, and derived the characteristic hyperbolic relationship between *V* and substrate concentration [*S*],

Department of Chemistry and Chemical Biology, Harvard University, Cambridge, MA 02138, USA, and Biodynamic Optical Imaging Center (BIO-PIC), Peking University, Beijing 100871, China. E-mail: xie@chemistry.harvard.edu



**Enzyme kinetics.** (A) Enzyme reaction velocity as a function of substrate concentration according to the Michaelis-Menten equation.  $K_M$  is the concentration at which the enzymatic velocity reaches half of its saturation value,  $V_{\max}$ . (B) Nonequilibrium steady-state condition of a single enzyme turnover experiment. The substrate and product concentrations are held constant during the reaction catalyzed by the enzyme. A similar situation exists in live cells.

$$V = \frac{V_{\max}[S]}{[S] + K_M} \quad (2)$$

where  $V_{\max} = k_{\text{cat}}[E]_T$  and  $[E]_T$  is the total enzyme concentration. At low  $[S]$ ,  $V$  is proportional to  $[S]$ , whereas at high  $[S]$ ,  $V$  saturates (see the figure, panel A).  $K_M$  is the substrate concentration at which the velocity is half of the saturation level (1). A more general derivation of the equation was subsequently given by Briggs and Haldane (3, 4).

The Michaelis-Menten equation not only quantified the kinetics of enzymatic reactions but also provided a practical means for characterizing an enzyme in terms of  $k_{\text{cat}}$  and  $K_M$ . A high  $k_{\text{cat}}$  and a low  $K_M$ , or a high  $k_{\text{cat}}/K_M$  ratio, are indicators for an enzyme's effectiveness. In 1934, Lineweaver and Burk showed how to rearrange the Michaelis-Menten equation to facilitate determination of  $K_M$  and  $k_{\text{cat}}$  by plotting  $1/V$  against  $1/[S]$  (5). The work was extremely highly cited, but in the computer era the significance of this rearrangement is less profound.

Many reactions do not follow the simple scheme of Eq. 1, and thus the "apparent"  $k_{\text{cat}}$  and  $K_M$  are not so simple to interpret. A major experimental advance in enzyme kinetics came in the 1970s and 1980s, when stopped-flow and continuous-flow experiments allowed the process of reaching the steady state to be studied. Using rapid sample mixing and high time resolution monitoring, these techniques allowed many complicated enzyme kinetic schemes to be decoded and many enzymatic intermediates to be determined (6).

Another major experimental advance came in the 1990s, when single-molecule

enzymology was made possible by single-molecule fluorescence imaging at room temperature and single-molecule manipulation (7, 8). The time traces of such experiments cannot be repeated, but their statistical properties are reproducible (9); similar observations have been made for the electric signals from a single ion channel (10), the first single-molecule experiment in biology. Over the past two decades, single-molecule enzymology has provided insights into how specific enzymes—particularly molecular motors and nucleic acid enzymes—work at the molecular level.

Single-molecule studies have also led to many insights that are general to all enzymes. One such general phenomenon is dynamic disorder. The  $k_{\text{cat}}$  of a single enzyme molecule is not a constant but rather exhibits large fluctuations (9, 11). The fluctuation of  $k_{\text{cat}}$  results from the fact that an enzyme has a broad distribution of interconverting and long-lived conformational states (12), each of which has a different  $k_{\text{cat}}$  (11, 13). This fluctuation in  $k_{\text{cat}}$  remains hidden in conventional ensemble experiments.

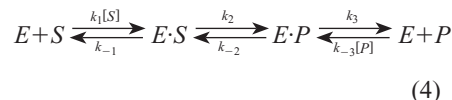
For the kinetic scheme in Eq. 1, single-molecule experiments have shown that the stochastic waiting time of an enzymatic reaction exhibits a distribution with an exponential rise followed by an exponential decay. For a single molecule with slowly interconverting conformational states with different  $k_{\text{cat}}$  and  $K_M$  (14), it follows that

$$\frac{1}{\langle \tau \rangle} = \frac{k_{\text{cat}}[S]}{[S] + K_M} \quad (3)$$

where  $\langle \tau \rangle$  is the mean of the stochastic

waiting time and the overbars denote the weighted averages of  $k_{\text{cat}}$  and  $K_M$  of different conformational states. Comparison with Eq. 2 shows that the Michaelis-Menten equation holds at the single-molecule level despite the ubiquitous and large fluctuations in  $k_{\text{cat}}$  (13). This result has been verified experimentally (11). This underscores why the Michaelis-Menten equation works so well at the ensemble level.

In single-molecule turnover experiments, each enzyme experiences constant substrate and produce concentrations in the volume of interest (dashed circle). Each enzyme is thus effectively in a non-equilibrium steady-state condition, which mimics the situation inside a live cell. Furthermore, many reactions in cells are reversible. In this case, the kinetic scheme underlying the Michaelis-Menten equation needs to be modified to allow for such reversibility:



Hill has shown how the forward and backward reaction fluxes ( $J^+$  and  $J^-$ , respectively) in a reversible enzymatic reaction can be related to the thermodynamic driving force (14, 15), namely the chemical potential difference,  $\Delta\mu$ , between product and substrate:

$$\Delta\mu = -kT \ln(J^+/J^-) \quad (5)$$

where  $k$  is the Boltzmann constant and  $T$  is the absolute temperature. Eq. 5 relates the enzymatic rate (that is, the difference between forward and backward fluxes) to chemical potential differences (which are determined by concentrations of reactants and products). In this sense, it is similar to the Michaelis-Menten equation, which relates enzymatic rates to substrate concentrations only. Equation 5 is more general than the Michaelis-Menten equation and is also more powerful, because it links the thermodynamic driving force to enzymatic kinetics. In the spirit of Michaelis and Menten, new experimental discoveries will no doubt lead to deeper understanding of enzyme kinetics and function, keeping scientists busy well into the next 100 years.

#### References and Notes

1. L. Michaelis, M. L. Menten, *Biochem. Z.* **49**, 333 (1913).
2. A. Cornish-Bowden, C. P. Whitman, *FEBS Lett.* **587**, 2711 (2013), special issue.

- G. E. Briggs, J. B. S. Haldane, *Biochem. J.* **19**, 338 (1925).
- Briggs and Haldane introduced the steady-state approximation,  $d[E\cdot S]/dt = 0$ . In a conventional enzymatic assay, the steady-state condition for  $E\cdot S$  is reached very rapidly because the amount of  $S$  is much greater than that of  $E$ , after which the  $E\cdot S$  concentration remains constant while the substrate concentration decreases and product concentration increases. The steady-state approximation results in the same form of the Michaelis-Menten equation as in Eq. 2 with  $K_M = (k_{cat} + k_{-1})/k_1$ . This derivation is presented in most textbooks on enzymes.
- H. Lineweaver, D. Burk, *J. Am. Chem. Soc.* **56**, 658 (1934).
- A. Fersht, *Structure and Mechanism in Protein Science, A Guide to Enzyme Catalysis and Protein Folding* (Freeman, San Francisco, CA, 1997).
- X. S. Xie, J. K. Trautman, *Annu. Rev. Phys. Chem.* **49**, 441 (1998).
- T. Funatsu, Y. Harada, M. Tokunaga, K. Saito, T. Yanagida, *Nature* **374**, 555 (1995).
- H. P. Lu, L. Xun, X. S. Xie, *Science* **282**, 1877 (1998).
- B. Sakmann, E. Neher, *Single-Channel Recording* (Plenum, New York, ed. 2, 1995).
- B. P. English *et al.*, *Nat. Chem. Biol.* **2**, 87 (2006).
- H. Yang *et al.*, *Science* **302**, 262 (2003).
- W. Min *et al.*, *J. Phys. Chem. B* **110**, 20093 (2006).
- T. L. Hill, *Free Energy Transduction and Biochemical Cycle Kinetics* (Dover, Mineola, NY, 2004).
- H. Ge, M. Qian, H. Qian, *Phys. Rep.* **510**, 87 (2012).

10.1126/science.1248859

## GEOCHEMISTRY

# Reformulating Table Salt Under Pressure

Jordi Ibáñez Insa

Sodium chloride (NaCl), the main component of table salt, is the archetypical ionic compound of chemistry textbooks. The large electronegativity difference between the participating elements drives salt formation. Metallic sodium transfers electrons to chlorine, and the resulting positively and negatively charged ions are held together by electrostatic attraction—ionic bonds. At ambient conditions, NaCl crystallizes in the so-called rocksalt structure, a cubic array of Na and Cl atoms in equal proportions (1:1 stoichiometry) and with six-fold coordination. With increasing pressure, a structural phase transition to the cubic, eight-fold coordinated NaCl-B2 phase is observed at  $\sim 30$  GPa [(1) and references therein]. Theory suggested that complete metallization of NaCl should occur above  $\sim 300$  GPa, and no Na-Cl compounds other than NaCl were known to exist. However, on page 1502 of this issue, Zhang *et al.* (2) show that stable Na-Cl phases with stoichiometries different from 1:1 and intriguing properties can be synthesized in the lab with high-pressure techniques.

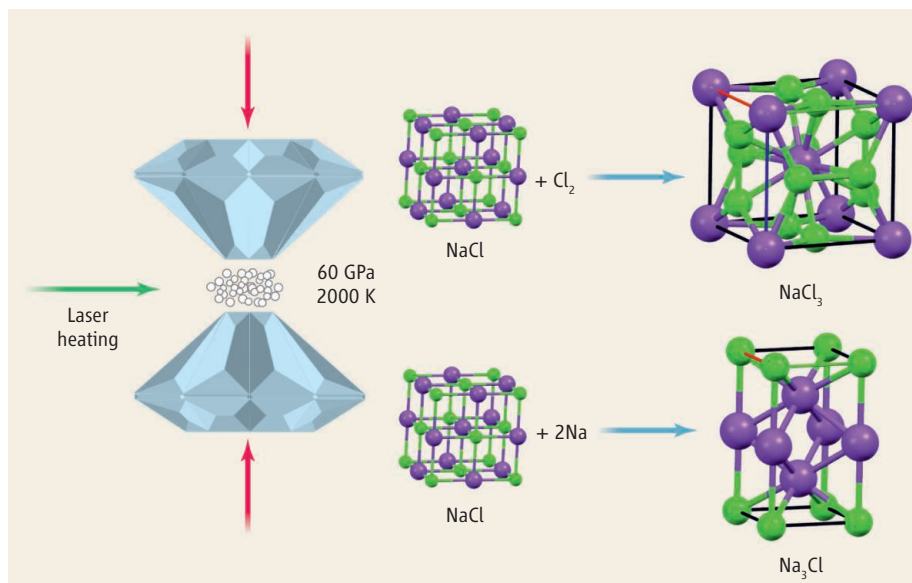
The application of high pressure allows researchers to dramatically change the bonding of atoms by reducing interatomic distances, and thus change the properties of solids. At sufficiently large pressures, insulators can become metals, soft chemical bonds become much stiffer, structural phase transitions take place, and chemical reactions that do not occur at ambient conditions become possible. By means of theoretical calculations with the *ab initio* evolutionary algo-

rithm USPEX (3), Zhang *et al.* predict that different Na-Cl compounds such as  $\text{Na}_3\text{Cl}$ ,  $\text{Na}_2\text{Cl}$ ,  $\text{Na}_3\text{Cl}_2$ ,  $\text{NaCl}_3$ , or  $\text{NaCl}_4$  are thermodynamically stable at nonambient pressure conditions. More important, they provide compelling experimental evidence that two of these compounds, most likely  $\text{NaCl}_3$  and  $\text{Na}_3\text{Cl}$ , are formed by squeezing NaCl in Cl- or Na-rich conditions in a diamond anvil cell and by applying temperatures around 2000 K with laser heating (see the figure).

In hindsight, one might be tempted to claim that the observation of new stoichiometries in the Na-Cl system is not that surprising. The argument could be something like “Compress a highly ionic substance and

Sodium chloride transforms into exotic compounds such as  $\text{NaCl}_3$  or  $\text{Na}_3\text{Cl}$  with compression, laser heating, and excess of Cl or Na.

you will end with covalent bonds and higher coordinations.” With increasing density upon compression, the inner electrons are expected to participate in the bonding process, making covalent bonds energetically more favorable. However, these new Na-Cl phases remain stable down to relatively low pressures (20 GPa for  $\text{NaCl}_3$ ). In addition, these phases exhibit remarkable crystal structures, chemical bonding, and electronic properties. Finally, the experimental confirmation of the theoretically predicted Na-Cl phases adds another success for USPEX, which shows an excellent ability to predict the stability of yet unknown compounds. The present results will surely stimulate both theoretical and experimental investi-



**Reformulating table salt.** When sodium chloride (NaCl) is squeezed by diamond anvils at high temperatures and under Cl- or Na-rich conditions, compounds such as  $\text{NaCl}_3$  or  $\text{Na}_3\text{Cl}$  can be formed. Zhang *et al.* theoretically predicted the stability of these phases and confirmed this prediction experimentally with x-ray diffraction and Raman-scattering measurements.

Institute of Earth Sciences Jaume Almera, CSIC, 08028 Barcelona, Catalonia, Spain. E-mail: jibanez@ictja.csic.es